



UNIVERSITÀ
DEGLI STUDI
FIRENZE

FLORE

Repository istituzionale dell'Università degli Studi di Firenze

Platelet-activating factor mediates an autocrine proliferative loop in the endometrial adenocarcinoma cell line HEC-1A.

Questa è la Versione finale referata (Post print/Accepted manuscript) della seguente pubblicazione:

Original Citation:

Platelet-activating factor mediates an autocrine proliferative loop in the endometrial adenocarcinoma cell line HEC-1A / M Maggi; L Bonaccorsi; G Finetti; V Carloni; M Muratori; G Laffi; M Serio; E Baldi.. - In: CANCER RESEARCH. - ISSN 0008-5472. - STAMPA. - 54:(1994), pp. 4777-4784.

Availability:

The webpage <https://hdl.handle.net/2158/371684> of the repository was last updated on

Terms of use:

Open Access

La pubblicazione è resa disponibile sotto le norme e i termini della licenza di deposito, secondo quanto stabilito dalla Policy per l'accesso aperto dell'Università degli Studi di Firenze (<https://www.sba.unifi.it/upload/policy-oa-2016-1.pdf>)

Publisher copyright claim:

La data sopra indicata si riferisce all'ultimo aggiornamento della scheda del Repository FloRe - The above-mentioned date refers to the last update of the record in the Institutional Repository FloRe

(Article begins on next page)

Platelet-activating Factor Mediates an Autocrine Proliferative Loop in the Endometrial Adenocarcinoma Cell Line HEC-1A¹

Mario Maggi, Lorella Bonaccorsi, Giovanna Finetti, Vinicio Carloni, Monica Muratori, Giacomo Laffi, Gianni Forti, Mario Serio, and Elisabetta Baldi²

Sezioni di Endocrinologia and Andrologia, Dipartimento di Fisiopatologia Clinica [M. Ma., L. B., G. F., M. Mu., G. F., M. S., E. B.] and Clinica Medica II [V. C., G. L.], Università di Firenze, 50134 Florence, Italy

ABSTRACT

We investigated the synthesis and biological effects of platelet-activating factor (PAF) in the human endometrial cancer cell line HEC-1A. We found that HEC-1A cells actively synthesize and release PAF, as demonstrated by both [³H]acetate incorporation into PAF and gas chromatography-mass spectrometry studies. HEC-1A cells not only synthesize but also respond to PAF. Indeed, in fura-2-loaded cells, PAF stimulates $[Ca^{2+}]_i$ increase with a median effective concentration of 5.6 nM. Furthermore, PAF induces a time-dependent expression increase of the nuclear protooncogene *c-fos* with a median effective concentration of 130 nM and stimulates DNA synthesis (median effective concentration, 700 nM). All of these effects are inhibited by the PAF receptor antagonist L659,989. Radioligand binding studies indicated the presence of two populations of PAF receptors with affinity constants in the nanomolar and micromolar range. Since the PAF antagonist *per se* inhibits DNA synthesis and cell proliferation, we suggest that PAF supports an autocrine growth circuit in HEC-1A cells. On the contrary, in the uterine leiomyosarcoma cell line SK-UT-1, which does not express specific binding sites for PAF, neither this phospholipid nor its receptor antagonist affect DNA synthesis. Our results provide evidence for the existence of an autocrine proliferative loop involving PAF in the endometrial cancer cell line HEC-1A.

INTRODUCTION

PAF³ is a potent, proinflammatory, ubiquitous lipid mediator (1, 2), chemically defined as 1-alkyl-2-acetyl-sn-glycero-3-phosphorycholine. Several lines of evidence suggest that PAF plays a significant paracrine role in stromal-epithelial cell interactions in the uterus, particularly during the implantation process (3). Indeed, although PAF synthesis is usually initiated in response to a variety of stimuli (2), a significant amount of this phospholipid has been found in rat uterus in the absence of any stimulation (4). In addition, human endometrial cells in primary culture synthesize PAF, both in basal conditions and following stimulation with progesterone (5, 6), whereas specific PAF binding sites are present in rabbit endometrium peaking during the periimplantation period (7–9).

Although an effect of PAF on cell proliferation has not been

Received 8/31/93; accepted 7/6/94.

The costs of publication of this article were defrayed in part by the payment of page charges. This article must therefore be hereby marked *advertisement* in accordance with 18 U.S.C. Section 1734 solely to indicate this fact.

¹This work was supported by Grant 92.02266 from the Consiglio Nazionale delle Ricerche (Progetto ACRO, Rome, Italy), by the Associazione Italiana Ricerca sul Cancro (Milano, Italy), and by the University of Florence. G. F. is a fellowship recipient of the Associazione Italiana Ricerca sul Cancro.

²To whom requests for reprints should be addressed, at Andrology Unit, viale Pieraccini, 6, 50139 Florence, Italy.

³The abbreviations used are: PAF, platelet-activating factor, 1-O-hexadecyl-2-acetyl-sn-glycero-3-phosphocholine; lyso-PAF, 1-O-hexadecyl-2-lyso-sn-glycero-3-phosphocholine; C-PAF, 1-O-hexadecyl-2N-methylcarbamyl-sn-glycero-3-phosphocholine; AM, acetoxymethyl ester; BAPTA, bis-(o-aminophenoxy)-ethane-N,N,N',N'-tetraacetic acid; TLC, thin-layer chromatography; acetyl-CoA, acetyl-coenzyme A; PC, phosphatidylcholine; BSA, bovine serum albumin; TBDSI, *tert*-butyldimethylchlorosilyl/imidazole; L659,989, (\pm)-trans-2-(3-methoxy-5-methylsulfonyl-4-propoxyphenyl)-5-(3,4,5-trimethoxyphenyl)tetraiodofuran; cDNA, complementary DNA; ATCC, American Type Culture Collection; PBS, phosphate-buffered saline; FCS, fetal calf serum; SIM, selected ion monitoring; $[Ca^{2+}]_i$, intracellular free calcium concentration; HEPES, 4-(2-hydroxyethyl)-1-piperazineethanesulfonic acid; SDS, sodium dodecyl sulfate; EC₅₀, median effective concentration; IC₅₀, 50% inhibitory concentration; PKC, protein kinase C.

precisely defined, recent data indicate that this phospholipid stimulates various intracellular signaling pathways linked to cellular proliferation, such as tyrosine phosphorylation (10–12) and mRNA transcription for the *c-fos* and *c-jun* oncogenes (12–16). In addition, ether lipids with structural similarity to PAF (17) and some PAF receptor antagonists (18, 19) are potent antiproliferative agents in several cancer cell lines.

The aim of the present study was to investigate production and biological activity of PAF in HEC-1A cells. We now report evidence for a PAF-driven autocrine loop critically involved in the regulation of proliferation of this endometrial cancer cell line.

MATERIALS AND METHODS

Chemicals. PAF, lyso-PAF, C-PAF, Fura 2/AM, A23187, ionomycin, BAPTA/AM, and propidium iodide were obtained from Calbiochem (La Jolla, CA). The sodium salt of [³H]acetic acid (1.9 Ci/mmol), [³H]acetyl-CoA (4 Ci/mmol), [³H]thymidine (2 Ci/mmol), and [³H]PAF (60 Ci/mmol) were purchased from New England Nuclear (Boston, MA). TLC phospholipid standards, PC, lyso-PC, phosphatidylethanolamine, phosphatidylserine, sphingomyelin, fatty acid-free BSA, EGTA, apidicolin, and RNase were from Sigma Chemical Co. (St. Louis, MO). Deutero-PAF was obtained from Cascade Biochem, Ltd. (Berkshire, United Kingdom). TBDSI reagent was from Alltech Applied Science (Deerfield, IL). High performance TLC silica gel 60 plates were from E. Merck (Darmstadt, Germany). Organic solvents were purchased from Carlo Erba (Milano, Italy). L659,989 was a generous gift from Merck, Sharp & Dhome (Rahway, NJ). bPc-fos(human)-1 cDNA probe was obtained from ATCC (Rockville, MD).

Cell Culture. HEC-1A and SK-UT-1 cells were obtained from ATCC. The HEC-1A *in vitro* cell line was established in 1968 by Kuramoto *et al.* (20) from explants of adenocarcinoma of human endometrium. The cells were grown in modified McCoy's 5A (Sigma) supplemented with 10% fetal calf serum (GIBCO, Grand Island, NY), penicillin (100 units/ml), streptomycin (0.1 mg/ml), and 2.2 g/l sodium bicarbonate as indicated by ATCC. Cultures were carried out in a humidified atmosphere of 5% CO₂-95% air at 37°C. Monolayers were split every 4–5 days using trypsin (0.05% in Mg²⁺- and Ca²⁺-free PBS containing 0.02% EDTA), and the culture medium was renewed every 2–3 days.

SK-UT-1 cells were isolated in 1972 from a human mixed uterine mesodermal tumor (leiomyosarcoma grade III). The cells were grown in Eagle's minimal essential medium with 10% FCS as indicated from the ATCC. These cells were used as control cells for [³H]thymidine incorporation and binding studies.

PAF Synthesis ([³H]Acetate Incorporation into PAF). [³H]PAF synthesis was measured by quantitative incorporation of [³H]acetate into PAF as described previously (21, 22). For these experiments, cells were grown to confluence on 6-well plastic plates, washed twice in serum-free McCoy's 5A medium containing 0.1% BSA, and preincubated in the same buffer in the presence of 50 μ Ci/well [³H]acetate. Stimuli were then added at the indicated concentrations for the established times. The reaction was stopped by adding 3 ml of ice-cold chloroform:methanol:acetic acid (1:2:0.04, by volume), and lipids were extracted twice in chloroform:methanol according to the Bligh and Dyer extraction procedure (23). The lower (chloroform) phases, containing the extracted lipids, were collected, washed once with methanol:water (10:9, v/v), evaporated under nitrogen, and redissolved in 200 μ l of chloroform:methanol (9:1, v/v). Samples were then applied on heat-activated high performance TLC silica gel 60 plates and developed in chloroform:methanol:water (65:35:6, by

volume). The labeled phospholipid products were identified by cochromatography with known standards. The R_f value of PAF was 0.2. The lipid fractions were visualized under an UV lamp after 2-p-toluidinylnaphthylene-6-sulfonate exposure; areas corresponding to PAF were carefully scraped, and the radioactivity was counted by liquid scintillation. For [^3H]PAF release experiments, lipids were separately extracted, as described above, from the conditioned medium and cell monolayers after the incubation procedure.

PAF acetyltransferase activity was assessed in lysates of HEC-1A cells by measuring the incorporation of [^3H]acetyl from radiolabeled acetyl-CoA into [^3H]PAF using lyso-PAF as substrate, as described previously (22, 24).

Identification of PAF-like Materials as Authentic PAF. We also performed gas chromatography-mass spectrometry analysis of PAF-like material extracted from HEC-1A cells preincubated with A23187 for 15 min by using a Perkin-Elmer 8420 gas chromatography-ion trap mass spectrometer (Perkin-Elmer, Norwalk, CO), as recently described (22). The phospholipids, extracted as described above, were reextracted from TLC powder, dried, and exposed to phospholipase C (10 units/ml) hydrolysis by shaking for three h in 1 ml 0.5 M Tris (pH 7.3) and 2.0 ml peroxide-free diethyl ether. The upper phase was evaporated, and the residue was dissolved in 100 μl of chloroform. One ml of *n*-hexane was added, and the solution was applied to a small glass column filled with 500 mg of silica gel, previously washed with 5 ml chloroform and 1 ml *n*-hexane. The sample was left at room temperature overnight in order to allow acetyl migration from position 2 to 3 of 1-*O*-radyl-2-acetyl glycerol (25). It was then washed with 4 ml *n*-hexane, eluted with 4 ml chloroform, collected in a reaction vial, and evaporated. The obtained diglyceride was then derivatized by adding 100 μl of TBDSI. The vial was capped and kept for 15 min at 100°C; after cooling, 0.5 ml of chloroform were added, and the mixture was washed with 2 ml of water. The lower phase was evaporated; then the residue was redissolved in 20 μl *n*-heptane and applied to the gas chromatograph-ion trap mass spectrometer. Chromatographic separation was obtained using a DB-1 (J&W, Rancho Cordova, CA) fused-silica capillary column (12 m \times 0.25 mm internal diameter; 0.25- μ film thickness). The oven temperature was programmed from 150°C (0.5-min hold) to 240°C at 20°C/min and 5°C/min up to 270°C. One 2- μl sample was injected in the splitless mode in a programmed temperature vaporizer (250°C). Helium was used as the carrier gas at 10 psi inlet pressure. Both full-scan mass spectra and SIM experiments were performed in the electron-impact mode at an ionizing energy of 70 eV. When analysis was performed with SIM, the ion m/e 415 (M-57), which is produced by cleavage of the *tert*-butyl radical from the parent ion, was selected. Full-scan spectra acquisition of internal standards were previously performed for ion mass assignments.

For quantitative analysis of PAF, standard curves were prepared combining PAF C:16 in the range 2–100 ng with 10 ng of deuterated internal standard and subjecting them to the derivatization procedure described above.

Calcium Experiments. For intracellular calcium measurements, cells were grown to confluence on plastic coverslips (Aclar; Allied Engineering Plastic, Pottsville, PA). During the 24 h before the experiments, cells were maintained in serum-free medium. $[\text{Ca}^{2+}]_i$ was determined using the calcium-sensitive dye Fura-2/AM as described previously (26). HEC-1A cells were loaded with 1 μM Fura-2/AM in the dark for 40 min at 37°C in serum-free McCoy's 5A; then the cells were washed and incubated for another 20 min in Fura-2-free medium. Cells were then washed with Krebs-Henseleit HEPES-KHH propidium iodide-free buffer (pH 7.4) containing 1.25 mM CaCl₂, 5.36 mM KCl, 0.81 MgSO₄, 130.62 mM NaCl, 5.55 mM glucose, 8.60 mM HEPES sodium salt, and 11.7 mM HEPES free acid. Coverslips were then mounted diagonally in a quartz cuvette so that the excitation and emission paths were at a 45° angle to the coverslip. The cuvette, containing 2 ml of KHH buffer, was maintained at 37°C. Fluorescence was measured using a spectrofluorometer (University of Pennsylvania Biomedical Group, Philadelphia, PA) using a single-wavelength excitation (340 nm)/emission (510 nm). Stimuli were added directly in the cuvette. Calibration was performed using ionomycin (0.02 mM) to obtain F_{\max} , followed by EGTA (8 mM) to obtain F_{\min} . Fluorescence measurements were converted to $[\text{Ca}^{2+}]_i$ according to Grynkiewicz *et al.* (27), assuming a K_d of Fura 2 for calcium of 224 nM.

RNA Analysis. For Northern analysis, HEC1-A cells were incubated with PAF, C-PAF, or L659,989 at the indicated concentrations and times in McCoy's serum-free medium. Total cellular RNA was prepared by the hot-phenol method (28) and quantitated by spectrofluorimetric analysis at 260 nm. Total cellular RNA (20 μg) was fractionated in a 1% agarose-formaldehyde gel and

then transferred overnight onto nylon membranes and baked at 80°C under vacuum for 2 h. Membranes were prehybridized for 1 h and then hybridized overnight at 65°C with a hybridization solution containing 10 mg/ml BSA, 7% SDS, 0.25 M Church and Gilbert buffer, 1 mM EDTA (pH 8), and 0.2 mg/ml hot-denatured sonicated herring sperm DNA. For RNA hybridization with the cDNA probe, a 1.3-kilobase gel-purified *Smal-HindIII* cDNA fragment for human *c-fos* protooncogene was used. The purified fragment was labeled with deoxycytidine 5'--[$\alpha^{32}\text{P}$]triphosphate by a nick translation kit (Promega, Madison, WI), chromatographed by Nu-Clean D50 Disposable Spun Columns (IBI, New Haven, CT), and denatured at 95°C for 10 min before use. After overnight hybridization, the membranes were washed three times with 1% SDS, 0.2 M Church and Gilbert buffer, and 0.1 mM EDTA (pH 8) at 65°C for 10 min. The nylon membranes were submitted to autoradiography using Kodak X-Omat AR film and Kodak X-Omatic regular intensifying screen at -80°C for 3 days.

Mitogenic Assay ([^3H]Thymidine Incorporation). For this set of experiments, cells were plated in 24-well plastic plates at the initial density of 10,000 cells/well in complete culture medium. After 2 days of culture, cells were maintained for 24 h in serum-free medium, and stimuli or vehicles (10 μl) were added at the indicated concentrations for the indicated times. All treatments were performed in triplicate. Cells were then incubated with [^3H]thymidine (1 $\mu\text{Ci}/\text{well}$) during the last 4 h of stimulation. Cells were washed twice with ice-cold 5% trichloroacetic acid and solubilized with 0.25 N NaOH in 0.1% SDS at 37°C for 20 min. Aliquots were transferred to plastic vials and counted by liquid scintillation.

For experiments on the effect of L659,989 on cell number, cells were plated at low density in 6-well plates, grown in complete culture medium, and treated in triplicate for 5 days with L659,989 (10 μM) in the same medium. Cells were trypsinized and counted with a Coulter Counter (Coulter Electronics, Ltd., Luton, United Kingdom).

Cell Cycle Analysis. HEC1-A cells (about 1.5×10^6) were cultured in 100-mm tissue culture plates in 10 ml complete culture medium for 12–18 h; then 5 $\mu\text{g}/\text{ml}$ of aphidicolin was added. After 24 h, partially synchronized cells were extensively washed in PBS, and 10 μM of L659,989 were added in 10 ml 10% FCS/McCoy's medium and incubated for the indicated times. After incubation, cells were washed twice with PBS, harvested using 3 ml trypsin/EDTA (0.05/0.02%) in PBS, and centrifuged at low speed. Cells were resuspended at 1×10^6 cells/ml in 2 ml of a fluorochrome solution containing 0.025 mg/ml propidium iodide, 0.025 mM EDTA, 0.015% Nonidet P-40, and 0.5 mg RNase in PBS. Samples were incubated in the dark at room temperature for 30 min and stored at 4°C until used for DNA analysis. Cell fluorescence was measured in a FACScan flow cytometer (Becton Dickinson, Mountain View, CA). The CELLFIT software was used to determine the distribution of cells in the various cell cycle compartments as G_0/G_1 , S, and G_2 .

Binding Experiments. HEC-1A cells were grown to confluence in 24-well plastic plates; 1.5×10^5 cells were incubated in binding buffer (PBS containing 3 mg/ml of free fatty acid BSA) at the indicated temperatures and for varying times. Cells were incubated in the presence of increasing concentrations of [^3H]PAF (0.6 nM–10 nM) without unlabeled ligands or fixed concentration (2 nM) of [^3H]PAF with increasing concentrations (1–100,000 nM) of unlabeled ligands. All of the measurements were obtained in triplicate. At the end of the incubation periods, the supernatants were removed, and the cells were washed six times in ice-cold Dulbecco-modified PBS containing 3 mg/ml BSA. Cells were then solubilized in 200 μl of 1% SDS containing 0.25 N NaOH, and 190 μl of the total volume were counted in a beta counter.

Statistical Analysis. The binding data were evaluated quantitatively with nonlinear least-squares curve-fitting using the computer program LIGAND. The program provides objective measures of goodness-of-fit and objective criteria for distinguishing between models of different complexity. The selection of the best model was based on comparison of the weighted sum of squares and/or the root mean square error. An F-test based on the "extra sum of squares" principle was used (29). The computer program ALLFIT (30) was used for the analysis of sigmoidal dose-response curves. This program uses the constrained four-parameter logistic model to obtain estimates of ED₅₀ and IC₅₀ values, the logit-log slope ("pseudo-Hill coefficient"), and relative potencies. Results are expressed as mean \pm SEM. Statistical comparisons were performed using unpaired Student's *t* test.

RESULTS

PAF Synthesis by HEC-1A Cells. Preliminary experiments performed in HEC-1A cell sonicates showed the presence of lyso-PAF: acetyl-CoA acetyltransferase activity in these cells. Lyso-PAF:acetyl-CoA acetyltransferase activity was time-dependent with a maximal activity at 15 min, followed by a plateau. PAF synthesis (measured as [³H]acetate incorporation into PAF) was assessed in intact HEC-1A cells, both in basal conditions and following stimulation with the calcium ionophore A23187 (1 μ M). [³H]Acetate incorporation into PAF in basal conditions was $26,282 \pm 2,302$ cpm/ μ g protein/60 min and was stimulated about 3-fold by a 1-h incubation with A23187 (84401 cpm/ μ g protein/60 min; $n = 4$). When lipids were separately extracted from cell pellets and supernatant, $60.3 \pm 10.4\%$ (in unstimulated) and $71.05 \pm 7.38\%$ (in A23187-stimulated cells) of [³H]PAF was found in the supernatant, indicating that part of the newly synthesized PAF was released into the medium by HEC-1A cells.

Identification of PAF Material Derived from HEC-1A Cells as Authentic PAF. Gas chromatography-mass spectrometry analysis of phospholipase C-treated and TBDMSI-derivatized PAF-like material comigrating with authentic PAF isolated from A23187-stimulated HEC-1A cells showed the presence of a chromatographic peak with identical retention time of deuterated standard PAF C16:0. Fig. 1 illus-

trates the full mass spectrum of TBDMSI derivatives of PAF extracted from HEC-1A cells (Fig. 1A) as well as for authentic PAF C16:0 (Fig. 1B). When monitored by SIM, the ion m/z 415 (M-57) of the material extracted from HEC-1A cells showed the same retention time as the PAF standard (not shown). These results indicate that 1-O-alkyl-sn-2-acetyl-glycerophosphocholine, the biologically active PAF, represents the predominant PAF species because the acyl-PAF analogue (1-O-acyl-sn-2-acetyl-glycerophosphocholine) has a different electron-impact mass spectrum and a different gas chromatographic retention time in our system. For quantitation of PAF, 16:0 deuterated-PAF was added to total HEC-1A lipids as internal standard, and after several purification procedures, the TBDMSI-derivatives were analyzed. The amount of 16:0 PAF in HEC-1A cells was estimated to be approximately 40 ng PAF/17.4 mg DNA/15 min incubation.

Effect of PAF on $[Ca^{2+}]_i$ in HEC-1A Cells. PAF induced a dose-dependent increase of $[Ca^{2+}]_i$ in Fura 2-loaded HEC-1A cells (Fig. 3A) with an apparent EC_{50} of 5.6 ± 0.7 nM ($n = 4$) and a maximal effect of $181 \pm 12\%$ increase over basal value. The increase of $[Ca^{2+}]_i$ appears to be mediated by specific PAF receptors, as the preincubation (2 min) with the PAF receptor antagonist L659,989 dose-dependently abolished the effect of 10 nM PAF (Fig. 2B) with an IC_{50} of 19 ± 1 nM ($n = 3$). The calcium increase in response to PAF (10 nM) was still present in the absence of extracellular calcium ($[Ca^{2+}]_e$, 0 + 4 mM EGTA), whereas it was completely abolished in cells simultaneously loaded with both Fura 2/AM and the intracellular calcium chelator BAPTA (Fig. 3A, inset). These findings suggest that the initial peak triggered by PAF is the result of a release of calcium from intracellular stores, whereas the sustained phase likely represents an influx of calcium from the extracellular medium.

Effect of PAF on c-fos mRNA Steady-State Levels. The effects of PAF (0.1 μ M) and its stable analogue C-PAF (0.1 μ M) on c-fos mRNA expression were assessed over a 2-h treatment period. The two phospholipids caused a significant increase in c-fos mRNA steady-state transcript levels (Fig. 3) at 15-, 30-, and 60-min treatments with a maximal increase in density of 22-fold at 30 min with PAF and of 28-fold at 60 min with C-PAF. The effect of PAF on c-fos gene expression was dose dependent (Fig. 4A) with an EC_{50} of 0.13 μ M and a maximal response (13-fold increase) at the concentration of 10 μ M. Coincubation with equimolar concentrations of the PAF antagonist L659,989 completely abolished the effect of 0.1 μ M PAF on c-fos mRNA steady-state transcript levels (Fig. 4B), suggesting the involvement of specific PAF receptors.

Effect of PAF and the PAF Receptor Antagonist L659,989 on Proliferation of HEC-1A Cells. Mitogenic assays of HEC-1A cells demonstrated a substantial increase of [³H]thymidine incorporation in PAF-stimulated cells after 24 h incubation. Such increase was dose dependent with an EC_{50} of 0.7 ± 0.2 μ M ($n = 5$) and a maximal effect of 3.92 ± 0.89 -fold increase over the basal state ($n = 5$). The effects of the two PAF precursors, lyso-PAF and lyso-PC, on DNA synthesis were also studied. We found that both lysophospholipids were able to stimulate [³H]thymidine uptake, although with lower potency than PAF. The EC_{50} for the 1-O-alkyl-PAF precursor lyso-PAF was 1.56 ± 0.2 μ M ($n = 3$), whereas the EC_{50} for the 1-O-acyl-PAF precursor lyso-PC was 12.5 μ M ($n = 2$). Conversely, treatment of the cells with the PAF receptor antagonist L659,989 dramatically decreased [³H]thymidine uptake. Such effect was already present after 16–18 h of treatment and peaked around 48 h (data not shown). The effect of L659,989 was dose dependent with an IC_{50} of 2.17 ± 0.7 μ M ($n = 6$) and a maximal inhibiting effect of about 90% obtained with 32 μ M. Both the proliferative effect of PAF and the antiproliferative effect of L659,989 were completely antagonized by concomitant incubation with equimolar concentrations of the two agents. Fig. 5

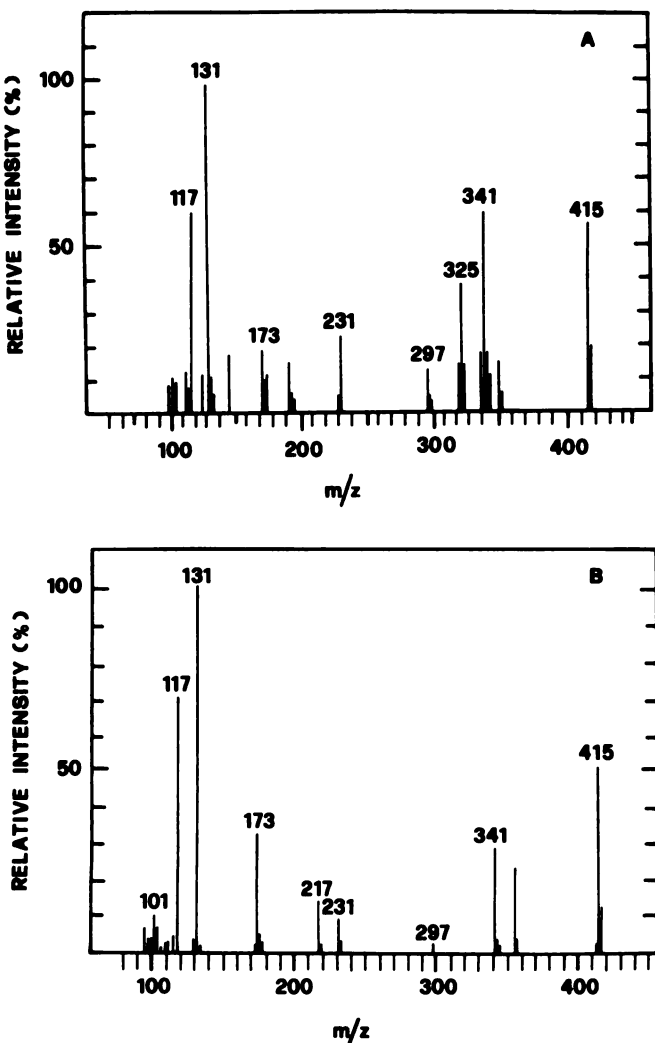


Fig. 1. Electron-impact mass spectra of the TBDMSI derivatives produced from HEC-1A-derived PAF-like material (A) and authentic PAF (B). The peak at m/z 415 represents the [M-57] ion for C16:0 ether.

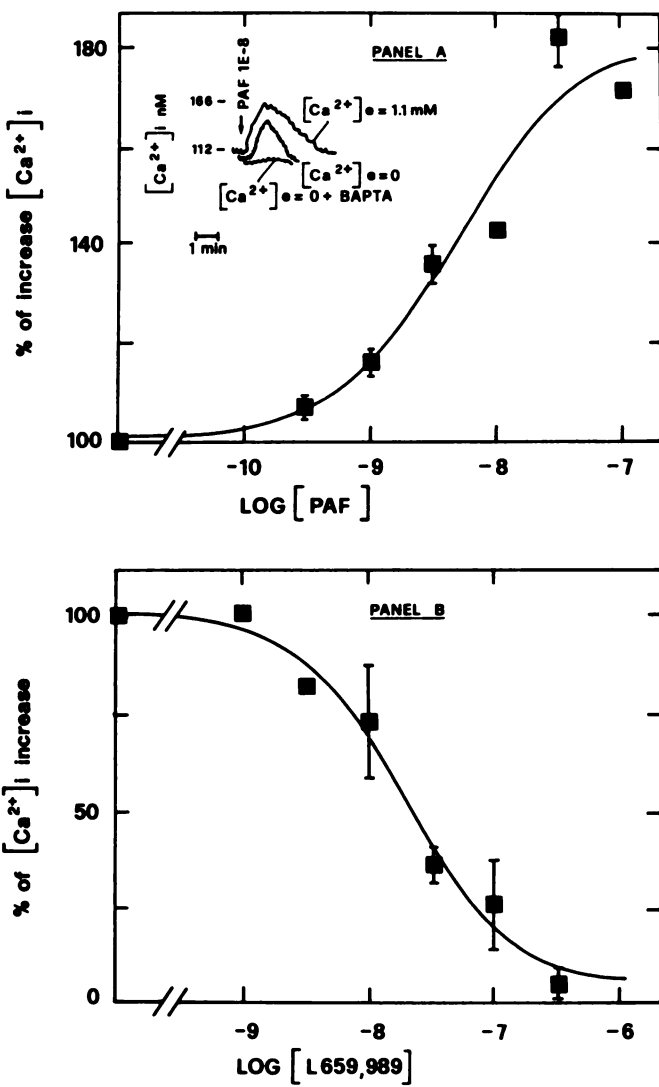


Fig. 2. Dose-response curve of PAF-mediated [Ca²⁺]_i increase in Fura-2 loaded HEC-1A cells (A). The EC₅₀ for PAF was 5.6 ± 0.7 nM ($n = 4$). Inset, representative tracings of PAF (10 nM)-stimulated Ca²⁺ increase in the presence and in the absence of extracellular calcium and in BAPTA-loaded cells. B, dose-response curve of inhibition of PAF (10 nM)-mediated Ca²⁺ increase after 2 min preincubation with the PAF antagonist L659,989. The IC₅₀ for this curve was 19 ± 1 nM ($n = 3$). Bars, SEM.

shows the result of a typical experiment on the effect of PAF and related compounds on DNA synthesis.

We also evaluated the effect of L659,989 on cell number by counting cells with a Coulter counter during 5 days of treatment. As shown in Fig. 6, these experiments confirmed cell growth inhibition by treatment with 10 μ M L659,989, starting from the first day of treatment. In addition, removing the PAF antagonist from the cells after 1 day of treatment by extensive washing with PBS and subsequent addition of complete medium (10% FCS) restored the cell number to the control value within 24 h, indicating a complete restoration of cell proliferation (not shown).

To study whether the antiproliferative effect of L659,989 on HEC-1A cells was due to a cytotoxic action, we evaluated the effect of 10 μ M L659,989 on cellular lactate dehydrogenase activity (assessed by an automatized colorimetric method) following 24 h of treatment. Lactate dehydrogenase cell content was not changed by the treatment with L659,989 (3854 ± 140.2 international units/well in controls versus 3813 ± 31.5 international units/well in treated samples; $n = 3$).

[³H]thymidine incorporation studies in SK-UT-1 cells after incubation (24–48 h) with PAF (0.1–10 μ M) and its antagonist L659,989 (0.1–10 μ M) did not show any modification of basal uptake with either agonist at any concentration tested ($n = 2$; data not shown).

Cell Cycle Analysis. To study the effect of L659,989 on the cell cycle, HEC-1A cells were synchronized by a 24-h exposure to 5 μ g/ml aphidicolin, a potent nonspecific inhibitor of DNA polymerase

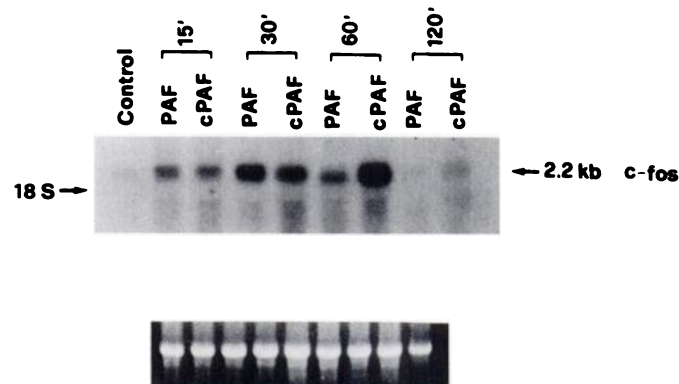


Fig. 3. Time course of PAF (0.1 μ M)-mediated and C-PAF (0.1 μ M)-mediated increase of c-fos mRNA steady-state transcript levels in HEC-1A cells. Ethidium bromide staining of total RNA loaded in each lane is shown below Northern blot.

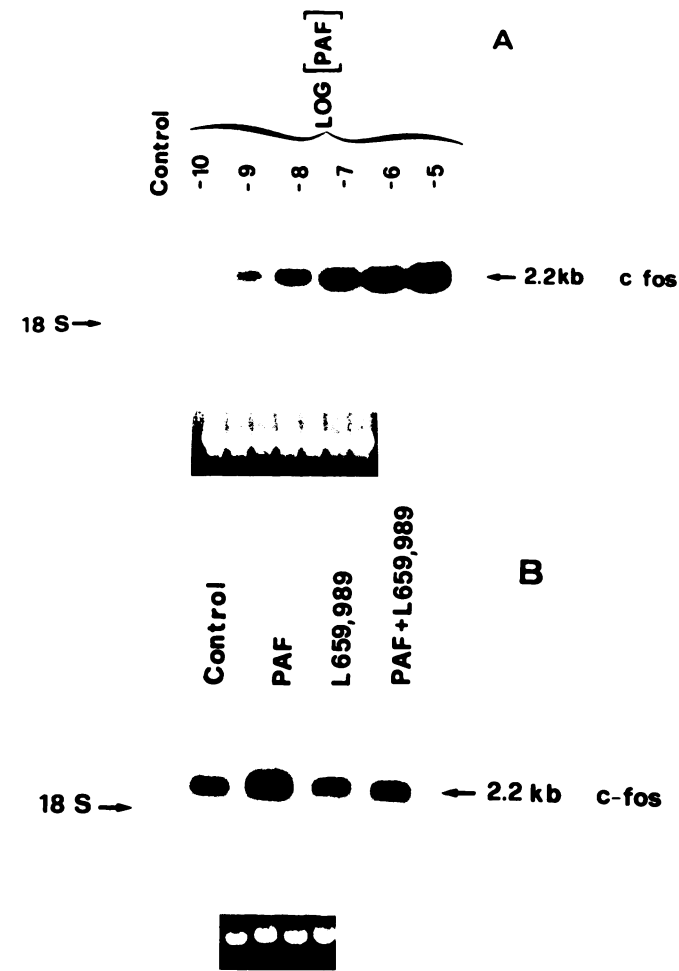


Fig. 4. A, dose-response curve of PAF-mediated increase of c-fos expression. B, effect of the PAF receptor antagonist L659,989 on PAF-induced increase of c-fos steady-state transcript levels. In both experiments, HEC-1A cells were incubated with the different agonists for 30 min. Ethidium bromide staining of total RNA loaded in each lane is shown below each Northern blot.

α (31). After such treatment, about 70% of the cells were in G_0/G_1 -early S, as indicated by fluorescence emission of propidium iodide-stained nuclei of the cells (not shown). Removal of aphidicolin (by extensive washing) allowed the cells to progress through the cell cycle. After a 4-h release from the aphidicolin block, the majority of the cells entered S, while 8 h later, most of the cells traversed G_2 -M. Eighteen h after aphidicolin release, the synchronized cells returned to G_0/G_1 and started to traverse S again. L659,989 treatment (10 μM) did not affect the cell cycle profile in the first 12 h. After 18 h, L659,989 caused a partial accumulation of the cells in the G_2 -M phase (Table 1). Thirty-six h after release from aphidicolin block, the PAF antagonist caused an accumulation into G_0/G_1 and a 50% reduction of S cells

Table 1 Effect of the PAF receptor antagonist L659,989 (10 μM) on cell cycle distribution of partially synchronized HEC-1A cell at 18 and 36 h after release from aphidicolin block

H after aphidicolin release	G_1	S	G_2/M
18	Control	44.58 \pm 3.55	11.54 \pm 0.35
	L659,989	35.78 \pm 1.52	10.81 \pm 0.24
36	Control	49.92 \pm 3.29	26.40 \pm 0.35
	L659,989	57.32 \pm 1.14	16.65 \pm 2.10 ^a

^a $P < 0.05$ versus control; $n = 3$ experiments.

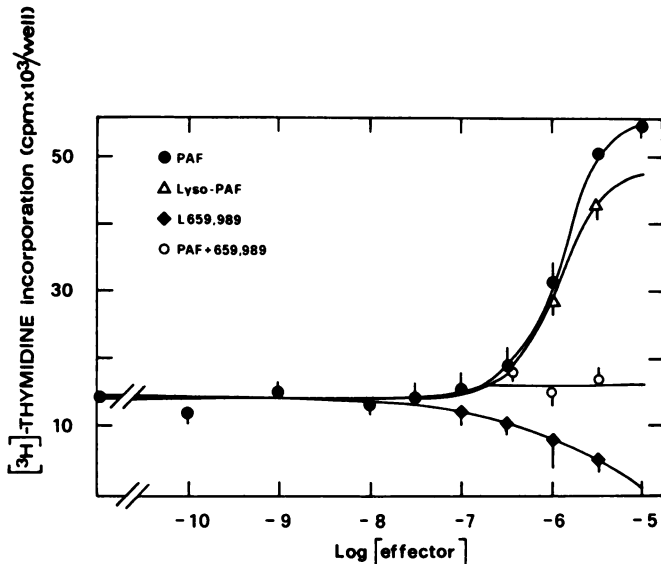


Fig. 5. Effect of 24-h treatment with increasing concentrations of PAF, lyso-PAF, L659,989, and the combination of equimolar concentrations of PAF plus L659,989 on $[^3\text{H}]$ thymidine uptake in HEC-1A. Results of a typical experiment (of at least three similar experiments performed in triplicate) are shown.

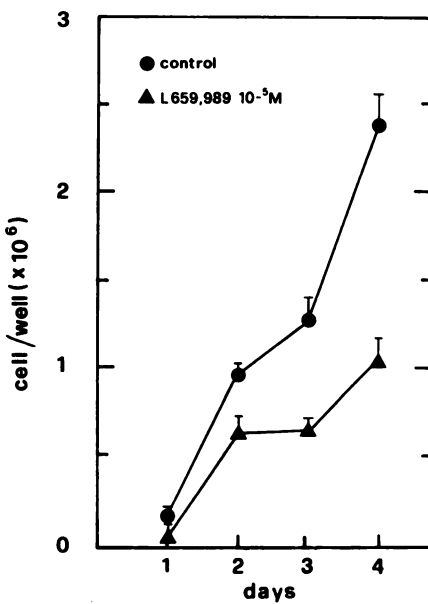


Fig. 6. Effect of the PAF antagonist L659,989 (10 μM) on HEC-1A cell number during 5 days of continuous treatment. Results are mean of triplicates of a representative experiment (of three similar experiments); bars, SEM. Cells were plated at the initial concentration of 50,000 cells/well.

over control values ($P < 0.05$; Table 1). Fig. 7 shows the result of a typical experiment.

Binding Studies. The binding reaction of $[^3\text{H}]$ PAF to HEC-1A cells was dependent on time and temperature. In contrast, the cell line SK-UT-1 did not bind $[^3\text{H}]$ PAF (data not shown). Specific $[^3\text{H}]$ PAF binding to HEC-1A cells was increasing as a function of time at 4, 22, and 37°C, reaching a maximum after 45 min at 37°C, 90 min at 22°C, and 24 h at 4°C (data not shown). Since the binding at 4°C was much more stable than in other experimental conditions, experiments were carried out at 4°C for 24 h.

Fig. 8A shows a typical family of competition curves among PAF, the PAF antagonist L659,989, and the PAF precursor lyso-PAF performed in HEC-1A cells. Using a subnanomolar (0.2 nM) concentration of the tracer to facilitate analysis of the high affinity portion of the curves, we obtained evidence for heterogeneity of the binding sites. Indeed, PAF and L659,989 competed for $[^3\text{H}]$ PAF binding in either nanomolar or micromolar concentrations, while the PAF precursor lyso-PAF displaced $[^3\text{H}]$ PAF only in the micromolar range. To further test the hypothesis that a heterogeneity of sites for PAF and L659,989 is present in HEC-1A cells, we generated multiple families of competition curves. Simultaneous computer analysis using the LIGAND program (29) was performed for 12 curves for a total number of 342 experimental determinations. Quantitative analysis indicated that a model involving only one site was severely inadequate. Introduction of a second independent class of sites significantly and dramatically improved the goodness-of-fit ($P \ll 0.0001$). Fig. 8, B and C, graphically shows the result of simultaneous modeling. The first site (R_1) is a low capacity site ($B_{max} = 269 \pm 183$ fmol/ 10^6 cells) that binds with nanomolar affinity PAF ($K_d = 1.7 \pm 1.6$ nM) and L659,989 ($K_d = 0.4 \pm 0.4$ nM). The second site (R_2) is a high capacity site ($B_{max} = 3.71 \pm 0.63$ nmol/ 10^6 cells) that binds with micromolar affinity PAF ($K_d = 9.7 \pm 1.45$ μM) and L659,989 ($K_d = 10.6 \pm 2$ μM).

When heterologous competition curves using lyso-PAF were included in receptor modeling, we found evidence for interactions of lyso-PAF only with the low affinity site, R_2 ($K_d = 4.8 \pm 1$ μM ; $n = 4$). Concerning R_2 , similar binding parameters were also obtained incubating HEC-1A cells in the presence of $[^3\text{H}]$ PAF and competitors at 22°C for 90 min. Since at this time and temperature PAF, L659,989 and lyso-PAF do not affect cell growth (data not shown), it is unlikely that binding parameters to R_2 could be affected by parallel changes in cell proliferation.

The statistical hypothesis that experimental data obtained in DNA synthesis or binding studies to R_2 using L659,989 share common IC₅₀s was tested by first forcing the curves to share this parameter and then by verifying that such constraint has minimal effect on several indicators of the goodness-of-fit, including the F ratio test (30). Since the F test was not significantly different from unity, it was derived that the shared parameter is compatible with each other ($P = 0.53$; mean IC₅₀, 7.5 \pm 2.5 μM).

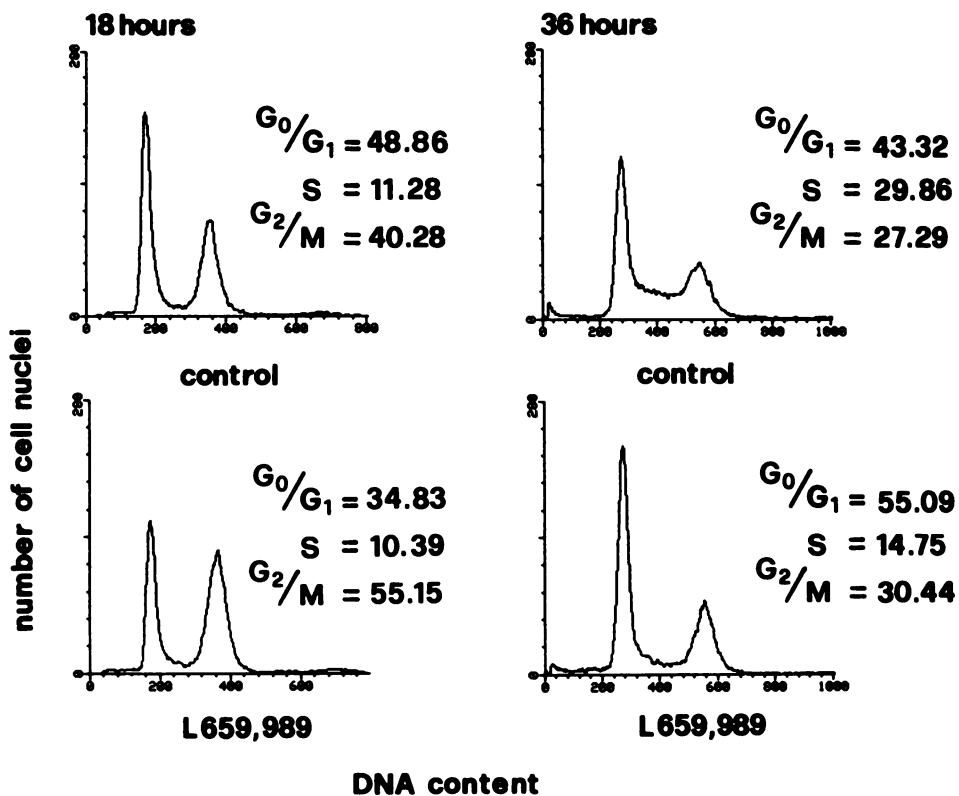


Fig. 7. Flow cytometric analysis of cell cycle distribution of synchronized HEC-1A cells 18 and 36 h after release from aphidicolin block and treatment with vehicle (first row) and L659,989 (10 μ M; second row). Representative tracings of three similar experiments.

DISCUSSION

This study strongly indicates that PAF supports an autocrine proliferative loop in the human endometrial cancer cell line HEC-1A. Indeed, we have shown that HEC-1A cells are both actively synthesizing and responsive to PAF in terms of $[Ca^{2+}]_i$, DNA synthesis, and expression of the protooncogene *c-fos*. In addition, the third generation PAF receptor antagonist L659,989 dramatically inhibits HEC-1A cell proliferation, further supporting the presence of an autocrine proliferative circuit. On the contrary, PAF or its antagonist L659,989 did not elicit any effect on thymidine uptake in the uterine leiomyosarcoma cell line SK-UT-1. Binding studies indicate that the biological effects of PAF and L659,989 are mediated by specific receptors present in HEC-1A cells and absent in SK-UT-1 cells.

Production of PAF by HEC-1A cells occurs at least through the anabolic, remodeling pathway of PAF synthesis, as demonstrated by the high [3 H]acetate incorporation into PAF both in basal conditions and following stimulation with the ionophore A23187. We have also shown that about 60% of newly synthesized [3 H]PAF is released into the cell-conditioned medium, suggesting the possibility of an autocrine action of this phospholipid. Moreover, gas chromatography-mass spectrometry analysis revealed that the large majority of PAF synthesized by HEC-1A cells consists of the biologically active PAF species 1-*O*-alkyl-*sn*-glycero-3-phosphocholine.

Addition of PAF to HEC-1A cells resulted in a rapid, dose-dependent and biphasic increase in $[Ca^{2+}]_i$. Such increase appears to be mediated by specific PAF receptors because it is inhibited by the PAF antagonist L659,989 and seems to involve both release of Ca^{2+} from intracellular stores as well as influx from extracellular medium. Furthermore, incubation with PAF resulted in a dose- and time-dependent increase of expression of the *c-fos* protooncogene. Induction of *c-fos* mRNA expression was inhibited by the PAF antagonist L659,989, again suggesting the involvement of a specific receptor. These results are in agreement with several other studies demonstrating an effect of

PAF on immediate-early gene expression (12–16). However, an effect of PAF on spontaneous cell proliferation has been reported only for Raji lymphoblasts, a Burkitt lymphoma-derived B-cell line (32), and guinea pig bone marrow cells (33). Moreover, the antiproliferative effect of some PAF receptor antagonists does not appear to be related to PAF receptors (18, 19). Therefore, we next investigated the effect of PAF and its receptor antagonist L659,989 on cell proliferation in order to demonstrate a mitogenic effect of this phospholipid in HEC-1A cells. We now report that PAF stimulates [3 H]thymidine incorporation in the HEC-1A cell line. Such stimulation was dose dependent and appears to be mediated by a PAF receptor, as demonstrated by the inhibition of this effect by equimolar concentrations of the antagonist L659,989. In addition, L659,989 strongly inhibited [3 H]thymidine uptake by these cells, and this effect was prevented by concomitant incubation with equimolar concentrations of PAF. These results strongly indicate, for the first time, the presence of a PAF-mediated autocrine loop, which appears to be critical for the progression of HEC-1A cells throughout the cell cycle. In fact, the antiproliferative effect of the PAF antagonist L659,989, assessed by studies on thymidine uptake and cell number, appears to be mediated by a relative accumulation of cells in G_2/M .

The different biological effects of PAF in HEC-1A cells ($[Ca^{2+}]_i$ increase, early oncogene expression, and DNA synthesis) have been obtained at different concentrations of the agonist, suggesting that calcium increase might be upstream to oncogene expression and DNA synthesis. On the other hand, PAF-mediated calcium signaling and mitogenesis in HEC-1A cells could be mediated by distinct subtypes of receptors. Indeed, we found the presence of two distinct classes of binding sites for [3 H]PAF in HEC-1A cells. The first site, R_1 , binds PAF and L659,989 in nanomolar concentrations, while the second one, R_2 , shows affinity in the micromolar range. The PAF precursor lyso-PAF apparently interacts only with the low affinity site, R_2 . The presence of high and low affinity binding sites for PAF has been

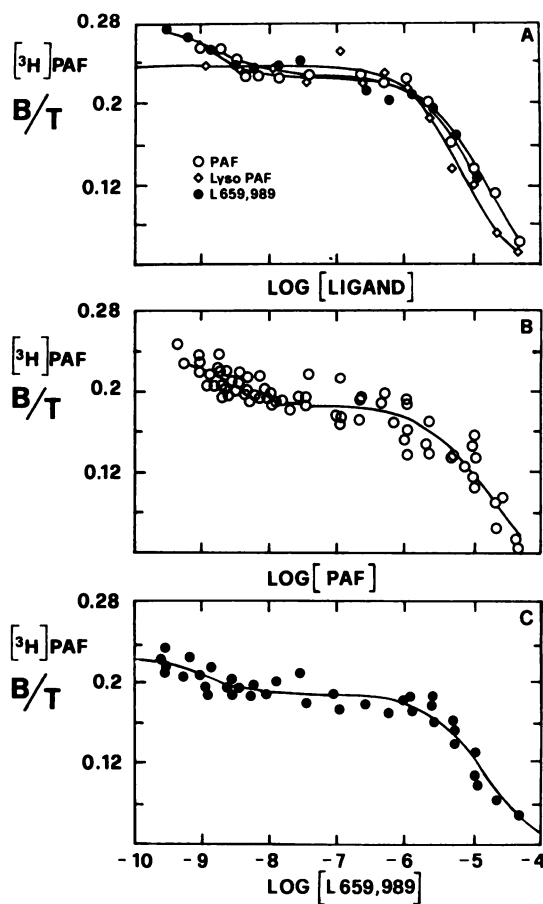


Fig. 8. Competition curves for PAF binding to HEC-1A cells. Ordinate, B/T; abscissa, total ligand concentration (labeled and unlabeled) on log scale. A, results obtained in a typical experiment using PAF (○), lyso-PAF (◇), and L659,989 (●) as competitors. B and C, results from 12 experiments analyzed simultaneously using a two-site model (29). Each point is the mean of triplicate determination.

reported previously in the pregnant rabbit uterus (7). Although it is difficult to stress which binding sites mediate the different biological effect of PAF, the effect of L659,989 on inhibition of DNA synthesis could be explained by binding to the low affinity site R₂. Hence, mitogenic effects could be dissociated from calcium fluxes, as recently reported for fibroblast growth factor receptors (34), suggesting interactions with other signaling pathways such as tyrosine kinase activation (34). PAF has been recently shown to increase tyrosine kinase activity both in platelets (19) and in proliferating cells (11, 12). In the A-431 epidermoid carcinoma cell line, PAF stimulation of c-fos expression involves both tyrosine kinase and PKC activation (12), although these effects appear to be dissociated from phospholipase C stimulation. Moreover, activation of tyrosine kinase seems to precede PKC activation (12). Preliminary data obtained in our laboratory also suggest a possible involvement of tyrosine kinase activation in the proliferative mechanism of PAF in HEC-1A cells.⁴

Interestingly, in HEC-1A cells as in rabbit endometrium, specific PAF binding was displaced by the PAF precursor lyso-PAF (7-9). Such finding might explain the increase of thymidine uptake detected in lyso-PAF-stimulated and, to a lesser extent, lyso-PC-stimulated HEC-1A cells. Indeed, although lyso-PAF is thought to be biologically inactive, a specific action in endometrial cells through PAF receptors is suggested (7, 8). It must be also stressed that lyso-PAF and other lysophospholipids have been reported to stimulate PKC activity directly (35); thus, a

proliferative action on HEC-1A cells through PKC activation cannot be excluded. An alternative explanation is given by the high intrinsic capacity of HEC-1A cells to produce PAF. Indeed, lyso-PAF might be metabolized by the cells to generate PAF which, in turn, stimulates cell proliferation and inhibits [³H]PAF binding.

In conclusion, we have shown evidence for the presence of an autocrine proliferative loop exerted by PAF in the human endometrial adenocarcinoma cell line HEC-1A. Additional studies will be necessary to establish a clinical implication of our finding.

ACKNOWLEDGMENTS

We are grateful to Professor Stefano Milani (Gastroenterology Unit, University of Florence) for expert advice and to Dr. William Parson (Merck, Sharp & Dohme Research Laboratories) for kindly providing the L659,989 compound.

REFERENCES

- Snyder, F. Biochemistry of platelet-activating factor: a unique class of biologically active phospholipids. *Proc. Soc. Exp. Biol. Med.*, 190: 125-135, 1989.
- Snyder, F. Platelet-activating factor and related acylated lipids as potent biologically active cellular mediators. *Am. J. Physiol.*, 259: C697-C708, 1990.
- Harper, M. J. K. Platelet-activating factor: a paracrine factor in preimplantation stages of reproduction? *Biol. Reprod.*, 40: 907-913, 1989.
- Yasuda, K., Satouchi, K., and Saito, K. Platelet-activating factor in normal rat uterus. *Biochem. Biophys. Res. Commun.*, 138: 1231-1236, 1986.
- Alecozay, A. A., Casslen, B. G., Riehl, R. M., Deleon, F. D., Harper, M. J. K., Silva, M., Nouchi, T. A., and Hanahan, D. J. Platelet-activating factor in human luteal phase endometrium. *Biol. Reprod.*, 41: 578-586, 1989.
- Alecozay, A. A., Harper, M. J. K., Schenken, R. S., and Hanahan, D. J. Paracrine interactions between platelet-activating factor and prostaglandins in hormonally-treated human luteal phase endometrium *in vitro*. *J. Reprod. Fertil.*, 91: 301-312, 1991.
- Kudolo, G. B., and Harper, M. J. K. Characterization of platelet-activating factor binding sites on uterine membranes from pregnant rabbits. *Biol. Reprod.*, 41: 587-607, 1989.
- Kudolo, G. B., and Harper, M. J. K. Estimation of platelet-activating factor receptors in the endometrium of the pregnant rabbit: regulation of ligand availability and catabolism by bovine serum albumin. *Biol. Reprod.*, 43: 368-377, 1990.
- Kudolo, G. B., Kasamo, M., and Harper, M. J. K. Autoradiographic localization of platelet-activating factor (PAF) binding sites in the rabbit endometrium during the peri-implantation period. *Cell Tissue Res.*, 265: 231-241, 1991.
- Dhar, A., and Shukla, S. D. Involvement of pp60^{c-src} in platelet-activating factor-stimulated platelets. *J. Biol. Chem.*, 266: 18797-18801, 1991.
- Chao, W., Liu, H., Hanahan, D. J., and Olson, M. S. Protein tyrosine phosphorylation and regulation of the receptor for platelet-activating factor in rat Kupffer cells. *Biochem. J.*, 288: 777-784, 1992.
- Tripathi, Y. B., Lim, R. W., Fernandez-Gallardo, S., Kandala, J. C., Guntaka, R. V., and Shukla, S. D. Involvement of tyrosine kinase and protein kinase C in platelet-activating-factor-induced c-fos gene expression in A-431 cells. *Biochem. J.*, 286: 527-533, 1992.
- Squinto, S. P., Block, A. L., Braquet, P., and Bazan, N. G. Platelet-activating factor stimulates a fos/Jun/AP-1 transcriptional signaling system in human neuroblastoma cells. *J. Neurosci. Res.*, 24: 558-566, 1989.
- Tripathi, Y. B., Kandala, J. C., Guntaka, R. V., Lim, R. W., and Shukla, S. D. Platelet-activating factor induces expression of early response genes c-fos and TIS-1 in human epidermoid carcinoma A-431 cells. *Life Sci.*, 49: 1761-1767, 1991.
- Schulam, P. G., Kuravilla, A., Putcha, G., Mangus, L., Franklin-Johnson, J., and Shearer, W. T. Platelet-activating factor induces phospholipid turnover, calcium flux, arachidonic acid liberation, eicosanoid generation, and oncogene expression in a human B cell line. *J. Immunol.*, 146: 1642-1648, 1991.
- Mazer, B., Domenico, J., Sawami, H., and Gelfand, E. W. Platelet-activating factor induces an increase in intracellular calcium and expression of regulatory genes in human B-lymphoblastoid cells. *J. Immunol.*, 146: 1914-1920, 1991.
- Berdel, W. E. Membrane-interactive lipids as experimental anticancer drugs. *Br. J. Cancer*, 64: 200-211, 1991.
- Berdel, W. E., Korth, R., Reichert, A., Houlihan, W. J., Bicker, U., Nomura, H., Vogler, W. R., Benveniste, J., and Rastetter, J. Lack of correlation between cytotoxicity of agonists and antagonists of platelet-activating factor (Paf-acether) in neoplastic cells and modulation of [³H]Paf-acether binding to platelets from humans *in vitro*. *Anticancer Res.*, 7: 1181-1188, 1987.
- Danhauser-Riedl, S., Felix, S. B., Houlihan, W. J., Zafferani, M., Steinhauser, G., Oberberg, D., Kalvelage, H., Busch, R., Rastetter, J., and Berdel, W. E. Some antagonists of platelet-activating factor are cytotoxic for human malignant cell lines. *Cancer Res.*, 51: 43-48, 1991.
- Kuramoto, H., Tamura S., and Notake, Y. Establishment of a cell line of human endometrial adenocarcinoma *in vitro*. *Am. J. Obstet. Gynecol.*, 114: 1012-1019, 1972.
- Baldi, E., Emancipator, S. N., Hassan, M. O., and Dunn, M. J. Platelet-activating

⁴ E. Baldi and M. Luconi, unpublished results.

- factor receptor blockade ameliorates murine systemic lupus erythematosus. *Kidney Int.*, **38**: 1030–1038, 1990.
22. Baldi, E., Faisetti, C., Krauzs, C., Gervasi, G., Carloni, V., Casano, R., and Forti, G. Stimulation of platelet-activating factor synthesis by progesterone and A23187 in human spermatozoa. *Biochem. J.*, **292**: 209–216, 1993.
 23. Bligh, E. G., and Dyer, W. J. A rapid method of total lipid extraction and purification. *Can. J. Biochem. Pharmacol.*, **37**: 911–917, 1959.
 24. Villani, A., Cirino, N. M., Baldi, E., Kester, M., McFadden, E. R., and Panuska, J. R. Respiratory syncytial virus infection of human mononuclear phagocytes stimulates synthesis of platelet-activating factor. *J. Biol. Chem.*, **266**: 5472–5479, 1991.
 25. Christian, B. W., and Blair, I. A. Analysis of platelet-activating factor in human saliva by gas chromatography mass spectrometry. *Biomed. Environ. Mass Spectrom.*, **18**: 258–264, 1989.
 26. Baldi, E., and Dunn, M. J. Endothelin binding and receptor down regulation in rat glomerular mesangial cells. *J. Pharmacol. Exp. Therap.*, **256**: 581–586, 1991.
 27. Grynkiewicz, G. M., Poenie, M., and Tsien, R. Y. A new generation of calcium indicators with greatly improved fluorescence properties. *J. Biol. Chem.*, **260**: 3440–3450, 1985.
 28. Sambrook, J., Fritsch, E. F., and Maniatis, T. *Molecular Cloning: A Laboratory Manual*. Cold Spring Harbor, NY: Cold Spring Harbor Laboratory, 1989.
 29. Munson, P. J., and Rodbard, D. LIGAND: a versatile computerized approach for characterization of ligand-binding systems. *Anal. Biochem.*, **107**: 220–239, 1980.
 30. De Lean, A., Munson, P. J., and Rodbard, D. Simultaneous analysis of families of sigmoidal curves: application to bioassay, radioligand assay, and physiological dose-response curves. *Am. J. Physiol.*, **235**: E97–E102, 1978.
 31. Huberman, J. A. New views of the biochemistry of eukaryotic DNA replication revealed by aphidicolin, an unusual inhibitor of DNA polymerase α . *Cell*, **23**: 647–648, 1981.
 32. Leprince, C., Vivier, E., Tretan, D., Galanaud, P., Benveniste, J., Richard, Y., and Thomas, Y. Immunoregulatory functions of Paf-acether. VI. Dual effect on human B-cell proliferation. *Lipids*, **26**: 1204–1208, 1991.
 33. Kato, T., Kudo, I., Hayashi, H., Onozaki, K., and Inoue, K. Augmentation of DNA synthesis in guinea pig bone marrow cells by platelet-activating factor (PAF). *Biochem. Biophys. Res. Commun.*, **157**: 563–568, 1988.
 34. Peters, K. G., Marie, J., Wilson, E., Ives, H. E., Escobedo, J., Del Rosario, M., Mirda, D., and Williams, L. T. Point mutation of an FGF receptor abolishes phosphatidylinositol turnover and Ca^{2+} flux but not mitogenesis. *Nature (Lond.)*, **358**: 678–681, 1992.
 35. Oishi, K., Raynor, R. L., Charp, P. A., and Kuo, J. F. Regulation of protein kinase C by lysophospholipids: potential role in signal transduction. *J. Biol. Chem.*, **263**: 6865–6871, 1988.